Constructing a Source Model Composed of Super Asperities for the 2011 off the Pacific Coast of Tohoku Earthquake

A. Nozu
Port and Airport Research Institute, Japan

SUMMARY:
A source model was newly developed for the 2011 off the Pacific coast of Tohoku, Japan, earthquake (M9.0) to explain strong ground motions. The source model involves 9 subevents with relatively small size, located off-the-coast of Miyagi through off-the-coast of Ibaraki. Strong ground motions due to the earthquake were calculated based on site amplification and phase characteristics, using the constructed source model. The agreement between the observed and calculated ground motions is quite satisfactory, especially for the velocity waveforms (0.2-1.0 Hz) including near-source pulses. The author refers to the small subevents as "super asperities" in this article based the work of Matsushima and Kawase (2006), because the size of the subevents used in this study is much smaller than the size of the "asperities" or "SMGAs" conventionally assumed for a huge subduction earthquake.

Keywords: The 2011 off the Pacific coast of Tohoku earthquake, strong ground motion, super asperity

1. INTRODUCTION

The 2011 off the Pacific coast of Tohoku, Japan, earthquake (hereafter referred to as "the Tohoku earthquake") is obviously the first M9 earthquake which was recorded by dense strong motion networks such as K-NET, etc (Kinoshita, 1998; Aoi *et al*., 2000). The occurrence of the earthquake enabled us to analyze real strong ground motions due to a M9 earthquake for the first time in the history. Before the occurrence of the earthquake, the author proposed the following for the evaluation of strong ground motions due to a large subduction earthquake (Nozu *et al*., 2006):
1) To use a source model composed of subevents with relatively small size.
2) To calculate strong ground motions based on site amplification and phase characteristics.
In the past study, the applicability of the above strategy was fully investigated for M8 class earthquakes (Nozu *et al*., 2006; Nozu and Sugano, 2008). In the present study, to investigate the applicability of the strategy for a M9 earthquake, a source model with subevents was newly developed for the 2011 Tohoku earthquake and simulation of strong ground motions was conducted based on the source model. To construct the source model, a forward modelling approach was used. The intention of the author was to develop a source model that can explain strong ground motions in the frequency range from 0.2-1 Hz, because strong ground motions in this frequency range have significant effects on a wide range of engineered structures including port structures.

The subevents used in this study are referred to as "super asperities" in this article based the work of Matsushima and Kawase (2006), because the size of the subevent used in this study is much smaller than the size of the "asperities" or "SMGAs" conventionally assumed for a huge subduction earthquake.

2. METHOD USED TO CALCULATE STRONG GROUND MOTIONS

For any candidate source model, strong ground motions were calculated based on site amplification and phase characteristics (Kowada *et al.*, 1998; Nozu *et al.*, 2006; Nozu and Sugano, 2008), which can

take into account the effect of sediments both on Fourier amplitude and Fourier phase of strong ground motions. Outline of the method can be described as follows.

The first step is to evaluate ground motions from a small event (Green's function). The Fourier amplitude of the Green's function is evaluated as a product of the source spectrum $|S(f)|$, the path effect $|P(f)|$ and the site amplification factor $|G(f)|$. The source spectrum is assumed to follow the ω^{-2} model (Aki, 1967). As for the path effect, geometrical spreading and nonelastic attenuation are considered (Boore, 1983). As for the site amplification factor, the empirical site amplification factor is used. As for the Fourier phase of the Green's function, the Fourier phase of an actual record at the site of interest is used. Thus, we can obtain a time domain Green's function which incorporates the effects of sediments both on Fourier amplitude and Fourier phase. The Green's function in the frequency domain can be written as follows:

$$|S(f)|\ |P(f)|\ |G(f)|\ O_s(f)\ /\ |O_s(f)|_p, \tag{2.1}$$

where $O_s(f)$ is the Fourier transform of an actual record at the site of interest and $|O_s(f)|_p$ is its Parzen-windowed amplitude (band width of 0.05 Hz is used). If several records are available at the site, it is recommended to choose an event which has a similar incident angle and a similar backazimuth with the target event. The second step is to superpose Green's functions to obtain strong ground motions from a large event (or a subevent of a large event) in the same way as the EGF method (e.g., Miyake *et al*., 2003). The resultant synthetic ground motions basically follow the ω^{-2} model.

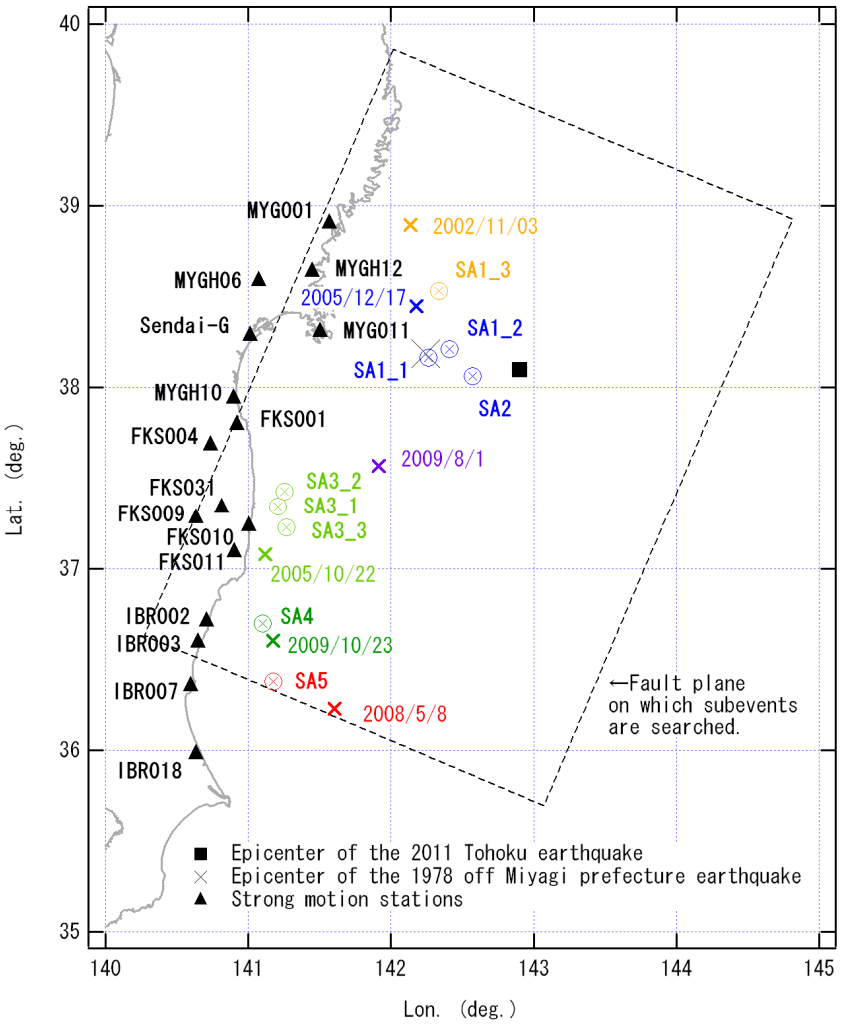

Figure 2.1. The proposed source model composed of nine super asperities. The triangles indicate strong motion stations. The crosses indicate epicentres of small events used to determine phase characteristics.

For the particular application to the Tohoku earthquake, the Q value estimated for the region (Satoh and Tatsumi, 2002) and the site amplification factors estimated based on spectral inversion technique (*e.g.*, Nozu and Nagao, 2005; Nozu *et al.*, 2006) were used. Some of the small events used to determine the Fourier phase of the Green's functions are shown in Fig. 2.1.

At two sites MYGH10 and FKS001, where the effect of soil nonlinearity was anticipated, the Green's functions were corrected for multiple nonlinear effects based on the simplified formula proposed by Nozu and Morikawa (2004) with nonlinear parameters (v_1, v_2)=(0.80, 0.008) for MYGH10 and (0.90, 0.005) for FKS001.

3. OFF MIYAGI PREFECTURE

The forward modelling was started with off Miyagi prefecture. Fig. 3.1 shows the observed ground velocities at three strong motion stations MYG011, MYGH12 and MYGH06 located in Miyagi prefecture. As already pointed out by many researchers (*e.g.*, Kurahashi and Irikura, 2011), strong ground motions in Miyagi prefecture include two distinctive wave packets, indicating contributions from at least two subevents. Then, as already done by other researchers (*e.g.*, Asano and Iwata, 2011), the locations and the rupture times of the subevents were determined based on the arrival times of the S waves corresponding to different wave packets (indicated by vertical red bars in Fig. 3.1). The estimated locations on the fault plane are indicated as "SA1_1" and "SA2" in Fig. 2.1 and Fig. 3.2. The estimated location of SA1_1 was close to the hypocenter of the 1978 off Miyagi prefecture earthquake (M7.4).

Then, assuming rectangular super asperities which involve the estimated locations as local rupture starting points, the parameters for the super asperities were determined through forward modelling approach. The estimated parameters include the length, the width, the seismic moment of the super asperities as well as the relative locations of the super asperities with respect to the rupture starting points. In the forward modelling approach, the parameters were determined so that the velocity waveforms in the strong motion stations in the frequency range from 0.2-1 Hz are reproduced as accurately as possible. Throughout the study, the rupture velocity was fixed to 3.0 km/s and the rise time was fixed to the width of the super asperity divided by the rupture velocity and multiplied by 0.25.

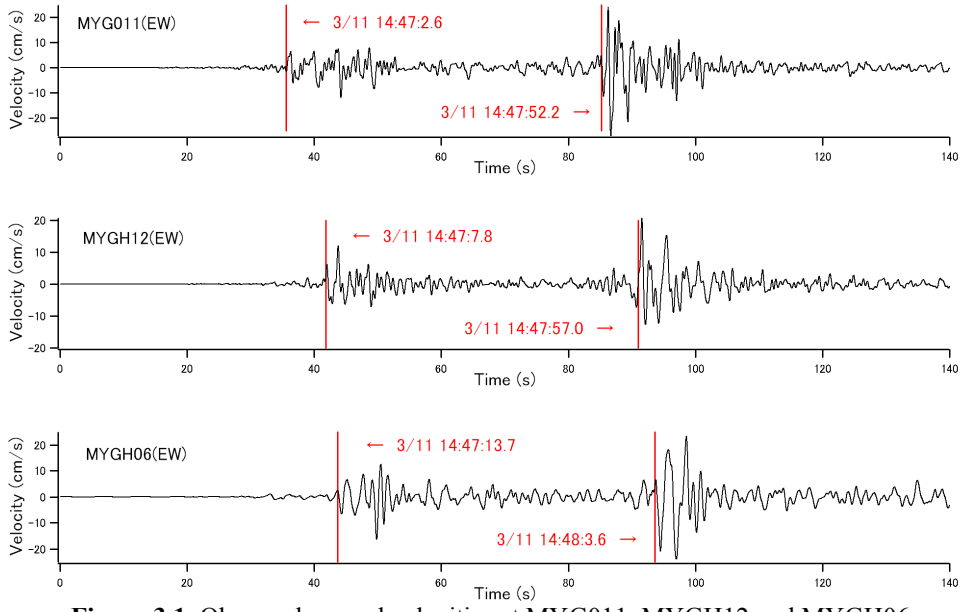

Figure 3.1. Observed ground velocities at MYG011, MYGH12 and MYGH06 (EW components; for MYGH12 and MYGH06, borehole records are shown)

Table 3.1. Parameters for the super asperity model.

	Rupture time (h:m:s)	Length (km)	Width (km)	Area (km^2)	M_0 (Nm)	Slip (m)	Rise time (s)
SA1_1	14:46:43.5	3.0	2.0	6.0	8.00E+18	28.3	0.17
SA1_2	14:46:46.9	4.0	3.0	12.0	8.00E+18	14.1	0.25
SA1_3	14:47:33.4	4.0	2.0	8.0	4.00E+18	10.6	0.17
SA2	14:47:26.3	3.5	3.0	10.5	2.10E+19	42.4	0.25
SA3_1	14:47:57.1	3.0	4.0	12.0	3.00E+18	5.3	0.33
SA3_2	14:48:04.4	3.0	4.0	12.0	3.00E+18	5.3	0.33
SA3_3	14:48:15.0	6.0	2.0	12.0	5.00E+18	8.8	0.17
SA4	14:48:25.8	8.0	3.0	24.0	9.00E+18	8.0	0.25
SA5	14:48:30.9	7.0	7.0	49.0	2.00E+19	8.7	0.58

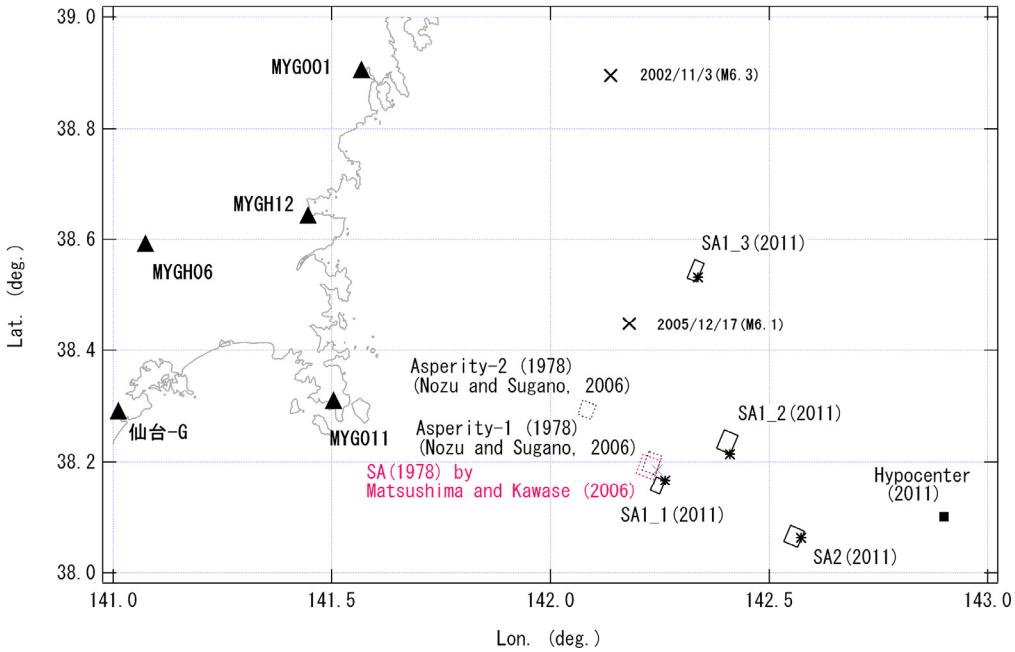

Figure 3.2. Detailed locations of four super asperities off Miyagi prefecture.

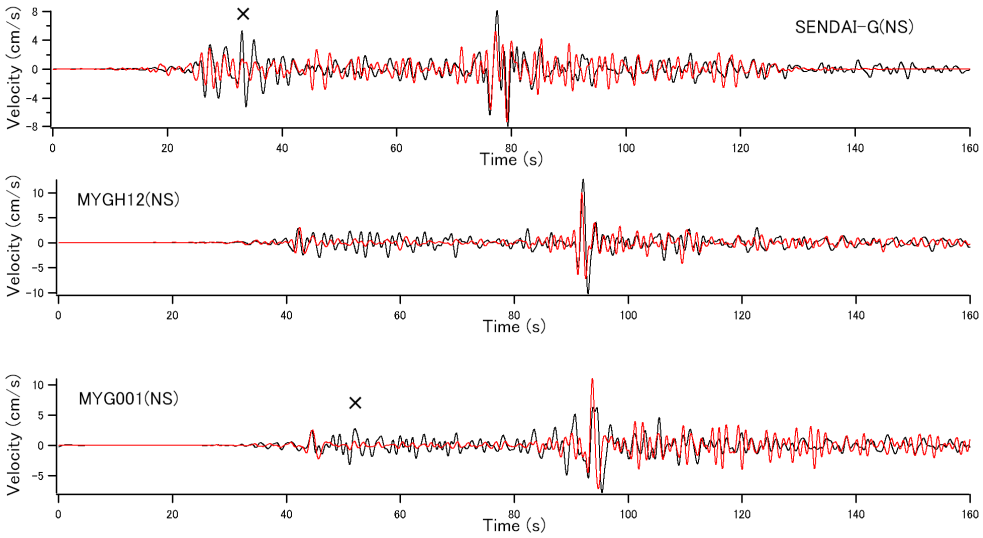

Figure 3.3. Observed (black) and synthetic (red) velocity waveforms (0.2-1 Hz). Contributions from SA1_1 and SA2 are considered in the synthetic waveforms.

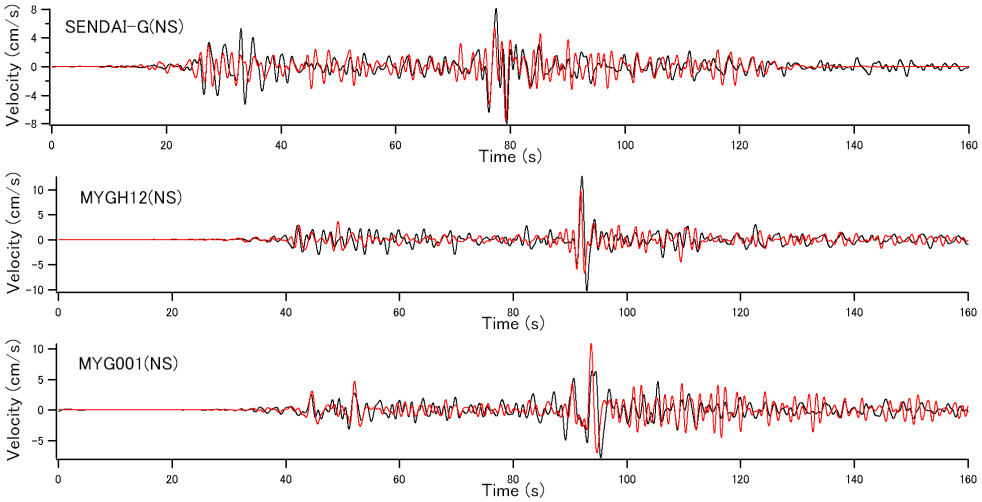

Figure 3.4. Observed (black) and synthetic (red) velocity waveforms (0.2-1 Hz). Contributions from four super asperities off Miyagi prefecture are considered in the synthetic waveforms.

The estimated parameters for SA1_1 and SA2 are listed in Table 3.1. The resultant waveforms, *i.e.*, the synthetic waveforms with contributions from two super asperities SA1_1 and SA2 are compared with the observed waveforms in Fig. 3.3. The agreement between the observed and synthetic waveforms is basically satisfactory. In particular, the amplitude and the width of S-wave pulses are reproduced very well, indicating that the estimated seismic moment and the size of the super asperities are appropriate (although different assumption on the rupture velocity may lead to different estimation of the size). In Fig. 3.3, however, some phases included in the observed waveforms are not included in the synthetic waveforms as indicated by crosses. To improve the results, two more super asperities SA1_2 and SA1_3 were introduced (Figs. 2.1 and 3.2). The synthetic waveforms with contributions from four super asperities agree quite well with the observed waveforms as shown in Fig. 3.4.

4. OFF FUKUSHIMA PREFECTURE

At stations around the border of Miyagi and Fukushima prefectures such as MYGH10 and FKS001, the contributions from four super asperities off Miyagi prefecture can almost explain the observed waveforms as shown in Fig. 4.1. At stations further south, however, the contributions from super asperities off Miyagi prefecture alone cannot explain the observed waveforms as shown in Fig. 4.2. In particular, three distinctive pulses are present in the observed waveforms as indicated by crosses, which do not appear in the synthetics. The locations and the rupture times of three super asperities corresponding to these pulses were estimated based on the arrival times of the S-waves. The estimated locations of the three super asperities, namely, SA3_1, SA3_2 and SA3_3 were close to the coast of Fukushima prefecture as shown in Fig. 2.1 and Fig. 4.3 (left). The parameters for the super asperities

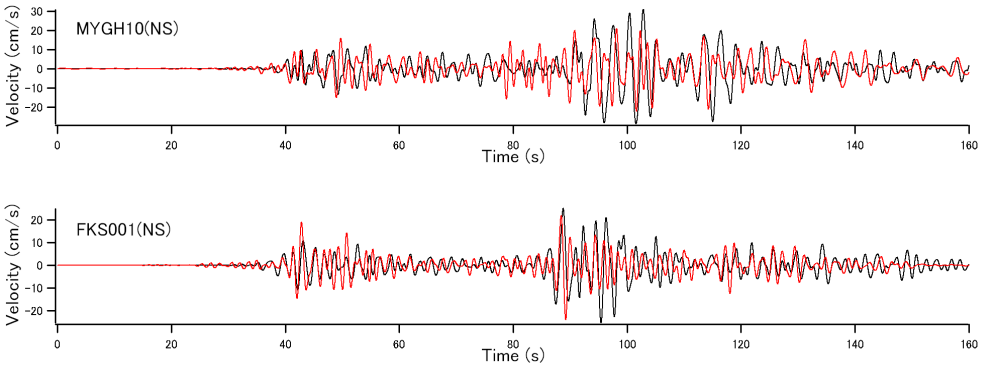

Figure 4.1. Observed (black) and synthetic (red) velocity waveforms (0.2-1 Hz). Contributions from four super asperities off Miyagi prefecture are considered in the synthetic waveforms.

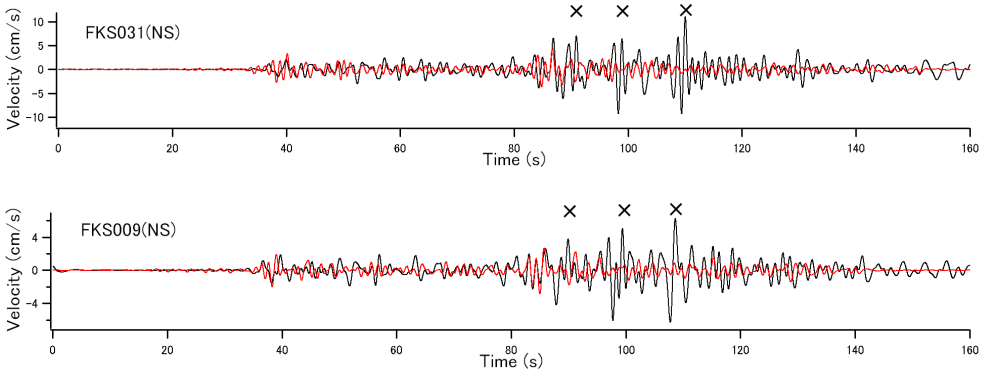

Figure 4.2. Observed (black) and synthetic (red) velocity waveforms (0.2-1 Hz). Contributions from four super asperities off Miyagi prefecture are considered in the synthetic waveforms.

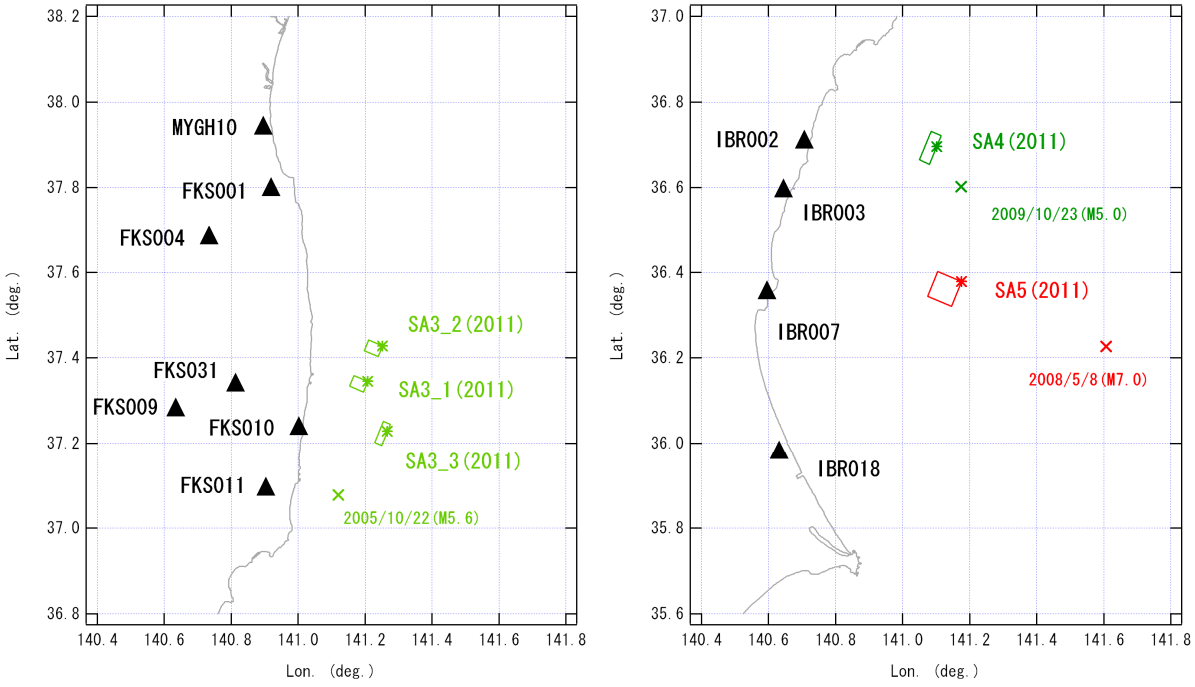

Figure 4.3. Detailed locations of super asperities off Fukushima (left) and off Ibaraki (right) prefectures.

were determined through forward modeling. The resultant parameters are given in Table 3.1. The synthetic waveforms with contributions from three super asperities off Fukushima prefecture are compared with the observed waveforms in Fig. 4.4. The agreement between the observed and synthetic waveforms is satisfactory.

5. OFF IBARAKI PREFECTURE

In Fig. 5.1, the synthetic waveforms with contributions from seven super asperities off Miyagi prefecture through off Fukushima prefecture are compared with the observed waveforms at two strong motion stations IBR002 and IBR003 located in northern Ibaraki prefecture. The synthetic waveforms can explain only the initial part of the observed ones, indicating the existence of another subevent which contributed to strong ground motions in the region. The location and the rupture time of the subevent, abbreviated as SA4, were estimated based on the arrival times of the S-waves. The estimated location of SA4 was close to the coast of Ibaraki prefecture as shown in Fig. 2.1 and Fig. 4.3 (right). The parameters for SA4 were determined through forward modeling. The resultant parameters are given in Table 3.1. The synthetic waveforms with contributions from seven super asperities off Miyagi

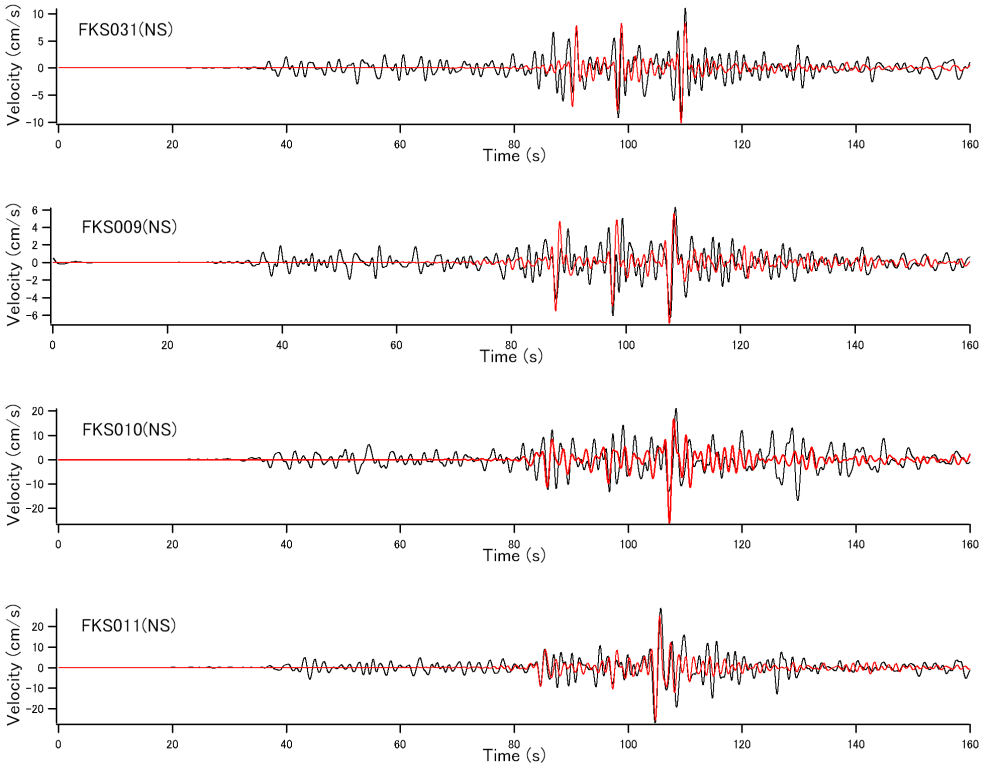

Figure 4.4. Observed (black) and synthetic (red) velocity waveforms (0.2-1 Hz). Contributions from three super asperities off Fukushima prefecture are considered in the synthetic waveforms.

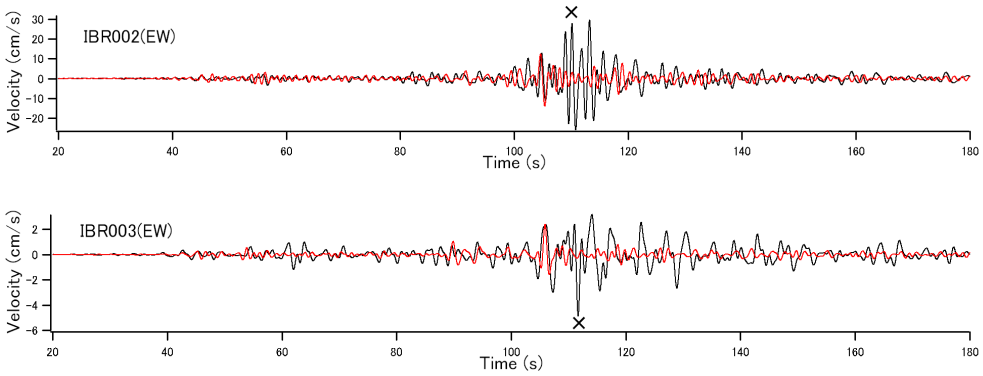

Figure 5.1. Observed (black) and synthetic (red) velocity waveforms (0.2-1 Hz). Contributions from seven super asperities off Miyagi through off Fukushima are considered in the synthetic waveforms.

prefecture through off Fukushima prefecture plus SA4 are compared with the observed waveforms in Fig. 5.2. The agreement between the observed and synthetic waveforms is satisfactory, not only at IBR002 and IBR003 but also IBR007.

At IBR018 located in southern Ibaraki prefecture, however, the synthetic waveforms from eight super asperities significantly underestimate the observed ones, indicating the existence of another subevent which contributed to strong ground motions in southern Ibaraki prefecture. The location and the rupture time of the subevent, abbreviated as SA5, were estimated based on the arrival times of the S-waves. The estimated location of SA5 was off the coast of Ibaraki prefecture as shown in Fig. 2.1 and Fig. 4.3 (right). The parameters for SA5 were determined through forward modeling. The resultant parameters are given in Table 3.1. The synthetic waveform with contributions from nine super asperities off Miyagi prefecture through off Ibaraki prefecture at IBR018 is compared with the observed waveform in Fig. 5.3. The agreement between the observed and synthetic waveforms was improved by introducing SA5. Results for other stations with nine super asperities can be found in our website at http://www.pari.go.jp/bsh/jbn-kzo/jbn-bsi/taisin/sourcemodel/somodel_2011touhoku.html.

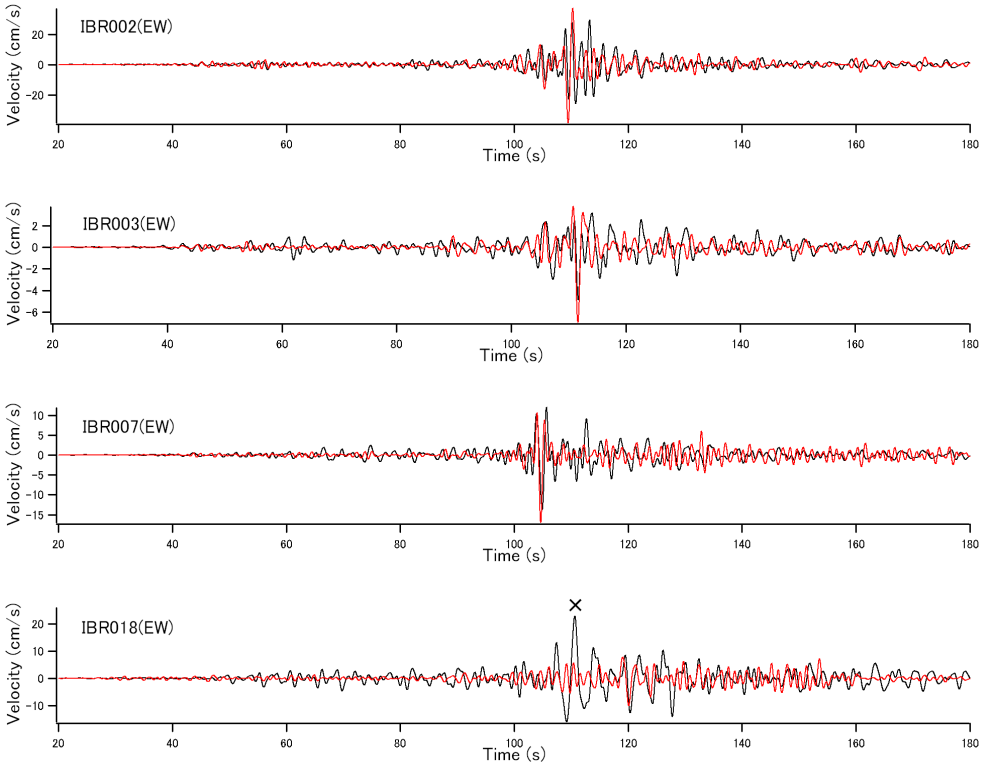

Figure 5.2. Observed (black) and synthetic (red) velocity waveforms (0.2-1 Hz). In addition to contributions from seven super asperities off Miyagi through off Fukushima, contributions from SA4 off Ibaraki are considered in the synthetic waveforms.

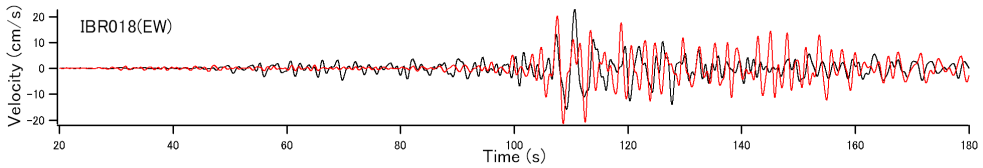

Figure 5.3. Observed (black) and synthetic (red) velocity waveforms (0.2-1 Hz). In addition to contributions from seven super asperities off Miyagi through off Fukushima, contributions from SA4 and SA5 off Ibaraki are considered in the synthetic waveforms.

6. DISCUSSION

One important character of the source model developed here is that the size of the subevent is significantly smaller than “asperities” or “SMGAs” conventionally assumed for a huge subduction earthquake. In fact, the dimension of the “super asperities” used in our analysis was around several kilo meters, while other authors (*e.g.*, Kurahashi and Irikura, 2011; Asano and Iwata, 2011) propose “asperities” or “SMGAs” with a dimension of several tens of kilo meters for the same event. It should be noted that the small size of the subevents used in this study is a natural reduction from the fact that, at many sites along the coast of Tohoku, strong motion pulses were observed and their pulse widths were around one to several seconds. As is well known, the duration of rupture of a subevent is related to the pulse width. If the dimension of a subevent is around several tens of kilo meters, then the pulse width will be more than 10 s and will not agree with the observed width. This is the reason why small subevents are needed to accurately reproduce strong ground motions in the frequency range from 0.2-1 Hz, which is of great importance from engineering point of view. Different assumptions on the rupture velocity may lead to different estimation of the size, but it will not significantly affect this conclusion.

Although the primary objective of the present source model is to explain strong ground motions in the frequency range from 0.2-1 Hz, it is basically applicable to higher frequencies. Fig. 6.1 shows the comparison of the observed and synthetic Fourier spectra (0.2-10 Hz) at selected sites. Fig. 6.2 shows the comparison of the observed and synthetic velocity envelopes (0.2-10 Hz) at the same sites. In these

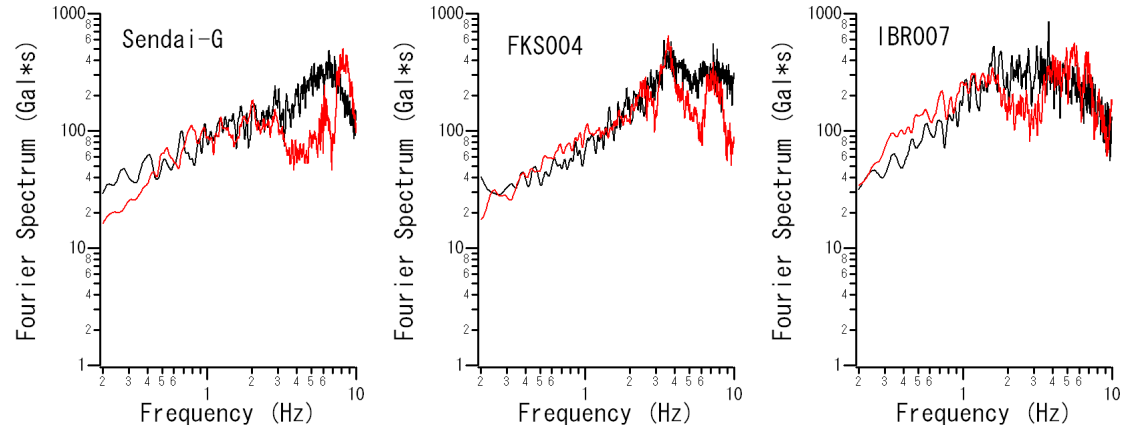

Figure 6.1. Observed (black) and synthetic (red) Fourier spectra (0.2-10 Hz). Contributions from nine super asperities off Miyagi through off Ibaraki are considered in the synthetic spectra. The spectra the composition of two horizontal components and smoothed with a Parzen window with a band width of 0.05 Hz.

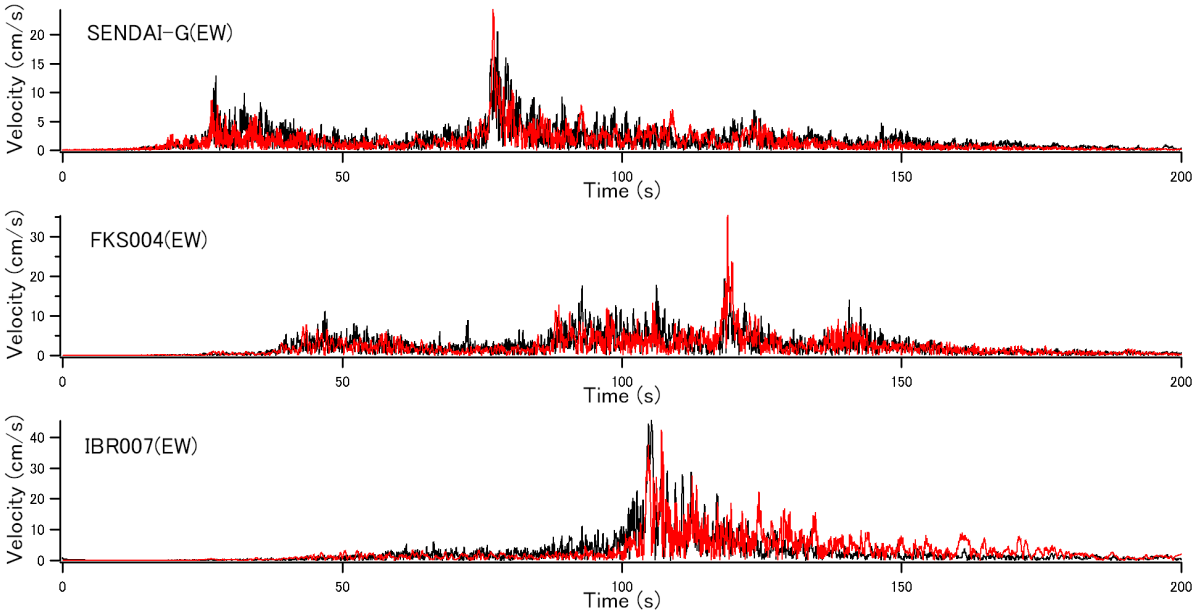

Figure 6.2. Observed (black) and synthetic (red) velocity envelopes (0.2-10 Hz). Contributions from nine super asperities off Miyagi through off Ibaraki are considered in the synthetic spectra.

figures, the synthetic waveforms were calculated considering nine super asperities. Basically, the agreement between the observed and synthetic Fourier spectra and velocity envelopes is satisfactory. Thus, the present model is basically applicable to high frequencies up to 10 Hz. In particular, the agreement in Fourier amplitude in Fig. 6.1 indicates that strong ground motions from subevents of a huge subduction earthquake follow the ω^{-2} model (Aki, 1967), because the simulation method used in this study is based on the ω^{-2} model.

7. CONCLUDING REMARKS

In the past study, the author proposed the following for the evaluation of strong ground motions due to a large subduction earthquake (Nozu *et al*., 2006):
1) To use a source model composed of subevents with relatively small size.
2) To calculate strong ground motions based on site amplification and phase characteristics.
The applicability of the above strategy was fully investigated for M8 class earthquakes (e.g., Nozu *et al*., 2006; Nozu and Sugano, 2008). In the present study, to investigate the applicability of the strategy

for a M9 earthquake, a source model with subevents was newly developed for the 2011 Tohoku earthquake. The constructed source model involves 9 subevents with relatively small size, located off-the-coast of Miyagi through off-the-coast of Ibaraki. Strong ground motions due to the earthquake were calculated based on site amplification and phase characteristics, using the constructed source model. The agreement between the observed and calculated ground motions was quite satisfactory, especially for velocity waveforms (0.2-1.0 Hz) including near-source pulses. The result definitely shows the applicability of the strategy for a M9 earthquake. The author refers to the small subevents as "super asperities" in this article based the work of Matsushima and Kawase (2006), because the size of the subevent used in this study is much smaller than the size of the "asperities" or "SMGAs" conventionally assumed for a huge subduction earthquake.

AKCNOWLEDGEMENT

The author would like to thank the National Research Institute for Earth Science and Disaster Prevention (NIED) for providing important strong motion data. The digital data of the site amplification factors and the computer program used to generate synthetics in this article including FORTRAN source code are open to public (Nozu and Nagao, 2005; Nozu and Sugano, 2008).

REFERENCES

Aki, K. (1967). Scaling law of seismic spectrum. *J. Geophys. Res.* **71**, 1217-1231.

Aoi, S., Obara, K., Hori, S., Kasahara, K. and Okada, Y. (2000). New strong-motion observation network: KiK-net. *Eos Trans. Am. Geophys. Union* **81**, 329.

Asano, K. and Iwata, T. (2011). Strong ground motion generation during the 2011 off the Pacific coast of Tohoku earthquake revealed by the broadband strong motion simulation. *The Seismological Society of Japan 2011 Fall Meeting*, A11-06 (in Japanese).

Boore, D.M. (1983). Stochastic simulation of high-frequency ground motions based on seismological models of the radiated spectra. *Bull. Seism. Soc. of Am*. **73**, 1865-1894.

Kinoshita, S. (1998). Kyoshin Net (K-net). *Seim. Res. Lett.* **69**, 309-332.

Kowada, A., Tai, M., Iwasaki, Y. and Irikura, K. (1998). Evaluation of horizontal and vertical strong ground motions using empirical site-specific amplification and phase characteristics. *J. Struct. Constr. Eng*., AIJ **514**, 97-104 (in Japanese with English abstract).

Kurahashi, S. and Irikura, K. (2011). Source model for generating strong ground motions during the 2011 off the Pacific coast of Tohoku Earthquake. *Earth Planets Space* **63**, 571-576.

Matsushima, S. and Kawase, H. (2006). Source model of a subduction zone earthquake with super-asperity. *Chikyu Monthly* S**55**, 98-102 (in Japanese).

Miyake, H., Iwata, T. and Irikura, K. (2003). Source characterization for broadband ground-motion simulation: kinematic heterogeneous source model and strong motion generation area. *Bull. Seism. Soc. Am.* **93**, 2531-2545.

Nozu, A. and Morikawa, H. (2004). Assessment of soil nonlinearity using empirical Green's function method. *Proceedings of 13WCEE*, No.2368.

Nozu, A. and Nagao, T. (2005). Site amplification factors for strong-motion sites in Japan based on spectral inversion technique. *Technical Note of the Port and Airport Research Institute*, No.1102 (in Japanese with English abstract).

Nozu, A., Nagao, T. and Yamada, M. (2006). Simulation of strong ground motions based on site-specific amplification and phase characteristics. *Third International Symposium on the Effects of Surface Geology on Seismic Motion*, Grenoble, France.

Nozu, A. and Sugano, T. (2008). Simulation of strong ground motions based on site-specific amplification and phase characteristics – accounting for causality and multiple nonlinear effects –. *Technical Note of the Port and Airport Research Institute*, No.1173 (in Japanese with English abstract).

Satoh, T. and Tatsumi, Y. (2002). Source, path and site effects for crustal and subduction earthquakes inferred from strong motions records in Japan. *J. Struct. Constr. Eng.*, AIJ **556**, 15-24 (in Japanese with English abstract).